Vlasov simulations of reconnection events and comparison with MMS

F. Califano[1], O. Pezzi[2], G. Cozzani[1,3], A. Retinò[3], F. Valentini[2], S.S. Cerri[4], G. Brunetti[2]

[1] Dip. di Fisica "E. Fermi", Univ. Pisa, Pisa, Italy
[2] Dip. di Fisica, Univ. Calabria, Arcavacata di Rende (CS), Italy
[3] CNRS, LPP UMR 7648, Ecole Polytechnique, France
[4] Department of Astrophysical Sciences, Princeton University, Princeton, NJ, USA

In this project we intend to set up a new model for the study of Magnetic Reconnection at electron scales. The model is based on the solution of the kinetic Vlasov equation for both electrons and protons using an Eulerian approach. These equations are coupled to the electromagnetic Maxwell equations in the so-called Darwin approximation which allows us to significantly increase the time step because light waves are cut off while all the main physics underlying the reconnection process are included. The use of an Eulerian approach instead of a more popular Lagrangian PIC approach is motivated by the very low noise of Eulerian Vlasov algorithms allowing to solve with high accuracy the fields, in particular the electric field even at very small scales. The price to pay for is the need of huge computational resources in terms of CPU time and memory. This project must be considered as the first step of a long time research project aimed at comparing observational data obtained from MMS measurements of reconnection in space and numerical simulations.

I. INTRODUCTION

Magnetic reconnection is a fundamental process during which a local change in the magnetic field topology leads to rapid dissipation of magnetic energy into kinetic energy and to a global rearrangement of the large scale magnetic connections. Due to the strong complexity of reconnection, numerical simulations represent a fundamental theoretical tool to study its dynamics. Experimental data are essential to validate numerical simulations as well as to provide realistic initial and boundary conditions. The synergy between simulations and experiments is therefore crucial. In-situ observations as, e.g. the Cluster mission, have been performed for decades leading to a good understanding of the physics of reconnection at fluid and ion scales, and MHD, two-fluid and hybrid simulations have supported such observations. On the other hand, the physics of reconnection at electron scales has been poorly understood until recent years when first attempts by Lagrangian PIC simulations have been performed. On the top of that, Space observations by the recently launched in 2015 Magnetopsheric Multi Scale (MMS) mission provide today fundamental experimental information on the physics at electron scales that was unachievable before even in the laboratory.

In this project we intend to address a key, yet poorly understood problem of electron-scale reconnection physics: how the electric field leading to reconnection onset is generated at reconnection sites. Addressing this problem requires the evaluation of the so-called Generalized Ohm's law. Our numerical approach is based on a Eulerian Vlasov-Darwin model to solve the protons and electrons Vlasov equation starting from observational data obtained from MMS measurements The numerical model integrates the Vlasov equation in the 3D-3V phase space, self-consistently coupled with the Maxwell equations in the *Darwin approximation* which separates the transverse and parallel component of the electric field in order to neglect the transverse displacement current. In practice we neglect light waves but take into account all the physical ingredients at play in reconnection dynamics.

We make use of an Eulerian approach characterized by a very low computational noise even at very small scales [1]. The code has been developed in collaboration with C. Cavazzoni and recently optimized for Marconi KNL.

The first part of the project has been supported by a INAF B computational grant, of strategic importance for code development and testing. Indeed it allowed us to start very rapidly our phase of code set up, testing and optimisation on Marconi KNL. It gave us the correct resources at the good time. This project has been crucial to apply for a INAF A call and ISCRA B call. A computational paper is in preparation. Possible developments of our research will potentially open the way for future PRACE call due to the very huge computational resources needed for a full Vlasov code.

II. THE DARWIN APPROXIMATION

We consider a non-relativistic electrons - protons plasma where particle collisions are negligible. The model equation is the Vlasov equations for both species coupled to the Maxwell system in the Darwin approximation [2] which, by cutting light waves, it allows to use "larger" time steps since any explicit scheme solving the full Maxwell equations would fulfill the CFL-like condition $\delta t \lesssim \delta x/c$ [3].

The Darwin approximation splits the electric field into a longitudinal (irrotational) and a transverse (solenoidal) component $= E_L + E_T$, where $\nabla \times E_L = 0$ and $\nabla \cdot E_T = 0$. Then, the transverse part of the displacement current in the Ampere equation is neglected. By using the electron mass m_e, the electron skin depth d_e, the inverse of the plasma frequency $\omega_{p,e}^{-1}$ and the light speed c as characteristic mass, length, time, and velocity, respectively, the dimensionless Vlasov-Darwin system of equations reads:

$$\partial_t f_\alpha + (v_\alpha \cdot \nabla) f_\alpha + \mu_\alpha (E + v_\alpha \times B) \cdot \nabla_{v_\alpha} f_\alpha = 0 \tag{1}$$

$$\nabla \cdot E_L = n\,; \quad \nabla \cdot B = 0 \tag{2}$$

$$\nabla \times E_T = -\partial_t B\,; \quad \nabla \times B = \partial_t E_L + j \tag{3}$$

where the electric and magnetic fields are normalized to $m_e c\omega_{p,e}/e$ and $\mu_\alpha = m_e/m_\alpha$. The number and current density, evaluated as $n = \sum_\alpha \int dv_\alpha f_\alpha$ and $j = \sum_\alpha \int dv_\alpha v_\alpha f_\alpha$, are normalized to $\bar{n}$ and $\bar{n}ec$, respectively.

Equations (2–3) can be further simplified. Following Ref. [4] we introduce an electrostatic potential ϕ such as $E_L = -\nabla\phi$. After some algebraic manipulations (see Ref. [5]), the final system of equations reads:

$$\nabla^2 \phi = -\sum n_\alpha\,; \quad \nabla^2 B = -\nabla \times j \tag{4}$$

$$\nabla^2 \hat{E}_T - \sum_\alpha \frac{n_{\alpha,0}}{\mu_\alpha} \hat{E}_T = [-\nabla \cdot \sum_\alpha \langle v_\alpha v_\alpha \rangle_\alpha + \\ + \sum_\alpha \mu_\alpha (n_\alpha E_L + \langle v_\alpha \rangle_\alpha \times B)] \tag{5}$$

$$\nabla^2 \Theta = \nabla \cdot \hat{E}_T\,; \qquad E_T = \hat{E}_T - \nabla\Theta \tag{6}$$

$$\nabla \cdot E_T = 0\,; \qquad \nabla \cdot B = 0$$

where $\langle h \rangle_\alpha = \int dv_\alpha f_\alpha h$ and $\nabla \cdot E_T = 0\,;\ \nabla \cdot B = 0$ represent a check of the correctness of the solution. We take the mean (constant) value for n_α in Eq. (5) in order to have constant coefficients in Eq. (5) (see Ref. [6] for the analogous approach when solving the Ohm's law including electron inertia).

III. VLASOV-DARWIN ALGORITHM AND CODE DESIGN

The Vlasov equations, Eqs. (1) with $a = e, p$, are integrated by adopting the splitting scheme in the e.m. limit [1]. Furthermore, assuming periodic boundary conditions in space, we integrate Eqs.(4)-(6) using the standard Fast Fourier Transform algorithm. We define Λ_x and Λ_v the space and velocity advection operators of the multi advection Vlasov equation [1] for the distribution function f_α^n (d.f.). Then the structure of the Vlasov-Darwin algorithm can be summarized as follows:

1. Performing the spatial advection $\tilde{f}_\alpha^n = \Lambda_x f_\alpha^n$;
2. Computing the moments of $\tilde{f}_\alpha^n$: n_α, $\langle v_\alpha \rangle_\alpha$ and $\langle v_\alpha v_\alpha \rangle_\alpha$; evaluating the electromagnetic fields E_L, E_T and B ;
3. Performing the velocity advection $f^{n+1} = \Lambda_v \tilde{f}_\alpha^n$.

Because of accuracy reasons, the x- and v-advection are shifted by $dt/2$. Both x- and v-advection require an interpolation of the d.f. (made by a 3^d order Van Leer scheme) corresponding to an upwind finite difference scheme.

The Vlasov equations are integrated in the phase space $D_{\mathbf{s}} \times D_{\mathbf{v}} = [L_x, L_y, L_z] \times [M_{vx}^\alpha, M_{vy}^\alpha, M_{vz}^\alpha]$, where $M_{vi}^\alpha = [-v_{\alpha,i}^{max}, v_{\alpha,i}^{max}]$, $\alpha = e, p$, respectively. We use $N_x \times N_y \times N_z$ grid points in space and $(2N_{\alpha,v_x} + 1) \times (2N_{\alpha,v_y} + 1) \times (2N_{\alpha,v_z} + 1)$ in velocity. We set $v_{\alpha,i}^{max}$ as a quite big multiple of the thermal speed $v_{th,\alpha}$ $(i = x, y, z)$ to ensure mass conservation (at least five). We take $m_p/m_e = 100$.

IV. CODE PERFORMANCE

The computational effort necessary to solve the Vlasov-Darwin system of equations, in particular the Vlasov equation in the 6-D phase space, is huge. The (x, y, z) space has been massively parallelized with MPI at Cineca in collaboration with C.Cavazzoni. The velocity space instead is all contained in each single processor. Here we present preliminary runs in 2D (x, y, v_x, v_y, v_z) of typical size of $1024^2 \times 51^2 \cdot 71$ for the electrons d.f. and $1024^2 \times 31^3$ for the protons d.f. corresponding to a memory requirement of about 50T which requires in turn at least 64 nodes. In Table

1 we list a number of 2D test run and run B is the reference one. We found that the best performance is obtained using 32 *task per node* for any given fixed number of nodes. A typical 2D run such as run B in Table 1 (with grid size as above) and about 10^4 steps would take in total about $36h$ corresponding on 64 nodes to a cost of about $0,15\,Mh$. We estimate 2D-3V production runs about $5 \div 10$ times longer, $T_{2D,\,prod} \simeq 0.8 \div 1.5 Mh$. From Table 1 we may state that: *i*) the best performance is obtained with 32 task per node independently of the total number of nodes, *ii*) the best performance is obtained by saturating at best the node memory, *iii*) there is a significant degradation of the performance for non power two number of grid points in space and when increasing the number of nodes. This last point is presently under investigation.

run	(N_x, N_y)	nodes	tsk/nd	r_1	r_2	t_{step}
A	(1024, 1024)	64	16	1	1	17.4
B	(1024, 1024)	64	32	1	1	12.9
C	(1024, 1024)	64	64	1	1	16.6
D	(1024, 1024)	128	16	1	0.5	11.2
E	(1024, 1024)	128	32	1	0.5	8.1
F	(1024, 1024)	128	64	1	0.5	10.9
G	(2560, 1280)	128	32	3.125	1.56	32.6
H	(3072, 1536)	256	32	4.5	1.125	24.7
I	(2048, 512)	64	32	1	1	14.3
J	(1664, 640)	64	32	1.02	1.02	16.3

Table I: Code performance, from left to right: run name, number of grid points in space, number of nodes, tasks per node, number of grid points normalized to run B (r_1), number of grid points per node normalized to run B (r_2), time per step in sec. More precisely: $r_{1,i} = N_{x,i}N_{y,i}/(N_{x,B}N_{y,B})$, $i = A, \dots J$. $r_{2,i} = r_{1,i}\, n_{nodes,B}/n_{nodes,i}$, $i = A, \dots J$. All runs have been performed on Marconi KNL, A2 partition, using $51^2 \cdot 71$ velocity points for the electrons and 31^3 for the protons.

V. NUMERICAL TESTS OF THE VLASOV-DARWIN CODE

We discuss now the results of numerical test compared to analytical solutions aimed at evaluating the capabilities of the numerical algorithm in describing the basic physics of collisionless plasmas.

A. Plasma waves and Landau damping

The first e.s. numerical test for a kinetic Vlasov code, not shown here, is given by the plasma waves dispersion relation and the associated Landau damping which becomes relevant when approaching wavelengths of the order of the Debye length $\lambda_{_D}$ corresponding to wave-vectors $k \gtrsim 2\pi/\lambda_{_D}$. We underline that Landau damping, in general hidden by the macro-partile noise in a PIC code, can play a key role in magnetic reconnection by providing the mechanism able to decouple the electrons from the magnetic field. The plasma waves test will be soon presented in a paper in preparation [5]. Here we just mention that all these test, dispersion relation and Landau damping, are in excellent agreement with standard textbooks analytical solutions.

B. Propagation and damping of whistler waves

We present a test for whistler waves at high frequencies where the main dynamics is driven by the electrons. Assuming the protons as a fixed neutralizing background, in the fluid limit the dispersion relation reads, in physical and dimensionless units:

$$\omega = \frac{\Omega_{ce} c^2 k^2}{\omega_{pe}^2 + c^2 k^2}\,; \qquad \omega = B_0 \frac{k^2}{1 + k^2} \tag{7}$$

where B_0 is the amplitude of the background magnetic field.

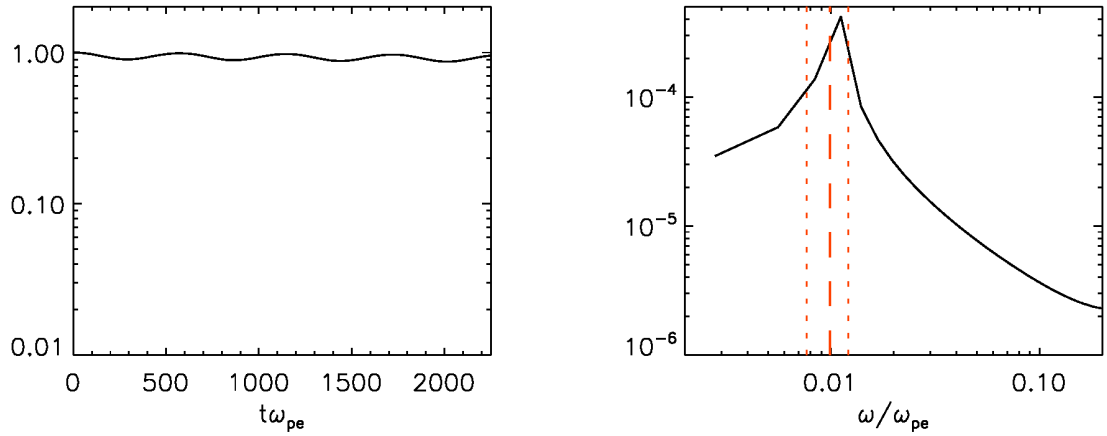

Figure 1: Left: Temporal evolution of the normalized mode m=1 amplitude, $\delta\hat{b}_y^1(t)$. Right: The squared amplitude of $\delta\hat{b}_y^1(\omega)$ vs. ω. The red solid line indicates the theoretical wave frequency $\omega = \omega_R$ while red dashed lines indicate the ω–resolution, i.e. $\omega = \omega_R \pm \Delta\omega/2$.

We performed a $1D$–$3V$ simulation with $B_0 = B_0 e_x$ and $B_0 = 1$, $L_x = 20\pi d_e$, $v_{e,i}^{max} = 10 v_{th,e}$ and $v_{p,i}^{max} = 7 v_{th,p}$ $(i = x, y, z)$. Note that it has been necessary to extend the velocity domain to ensure mass conservation in the simulation. The phase space has been discretized with $N_x = 128$, $N_{e,v_x} = N_{e,v_y} = N_{e,v_z} = 101$ for the electrons and $N_{p,v_x} = N_{p,v_y} = N_{p,v_z} = 71$ for the protons. We also set $m_p/m_e = 1836$, $T_e/T_p = 1$, $v_{th,e}/c = 10^{-3}$.

In Fig.1, left frame, we show the temporal evolution of the (normalized) mode amplitude $m = 1$ of the y-component of the magnetic field, $\delta\hat{b}_y^1$, obtained by a Fourier transform in space. We see that the mode oscillates in time without any significant damping for about four periods. In the right frame, we show the same quantity squared vs the frequency ω resulting from a Fourier transform in time. We see that the mode frequency well agrees with the theoretical expectation in the limit of the resolution in frequency.

C. Magnetic Reconnection

We initialise the code using a force balance initial equilibrium at electron scales obtained by including the electron FLR effects. These are the first important kinetic effect in order to maintain the equilibrium on a time scale larger than that for the development of reconnection [7]. The initial equilibrium profile for the magnetic field and the density field, see Fig.2 left column, is chosen as to mimic the electron diffusion region observed by MMS during a magnetopause crossing (27/01/2017 around 12.45 UTC). We take the magnetic field reversal of characteristic width $L_{eq} \simeq 6 d_e$ in agreement with MMS data and a second field reversal much smoother, $L_{junct} \simeq 36 d_e$ in order to fulfil the periodicity boundary conditions but sufficiently smooth as to slow down reconnection with respect to the main current sheet. The density profile is obtained by fitting the asymptotic MMS data and imposing force balance. Both profiles turn out to be asymmetric, as typically observed at the magnetopause. Electron and proton temperatures are kept constant $T_e = 1$, $T_p = 1$. We apply a small initial perturbation to the electron distribution function in order to trigger reconnection. We present here preliminary results of a $2D$-$3V$ simulation with $L_x = 240\pi d_e$ and $L_y = 120\pi d_e$. The numerical grid is given by $N_x = 2048, N_y = 1024$, $N_{e,v_x} = N_{e,v_y} = 51$, $N_{e,v_z} = 71, N_{p,v_x} = N_{p,v_y} = N_{p,v_z} = 31$. The simulation runs on 128 nodes of KNL which is the minimum size because of the memory requirements for the electron and proton d.f. We use a mass ratio $m_p/m_e = 100$ and an electron thermal velocity $v_{th,e}/c = 0.05$. In Fig.2 central and right columns, we plot the flux function ψ at different time instants. We see the progressive formation of an asymmetric magnetic island. At our knowledge this is the first Vlasov simulation of electron magnetic reconnection.

VI. CONCLUSION

We have started a new project of kinetic electron reconnection by means of a Vlasov code and using space data available from the MMS mission. The code has been build up recently and has been implemented on Marconi KNL thanks to an initial INAF B computational grant. The rapidity and efficiency of the INAF grant system has been

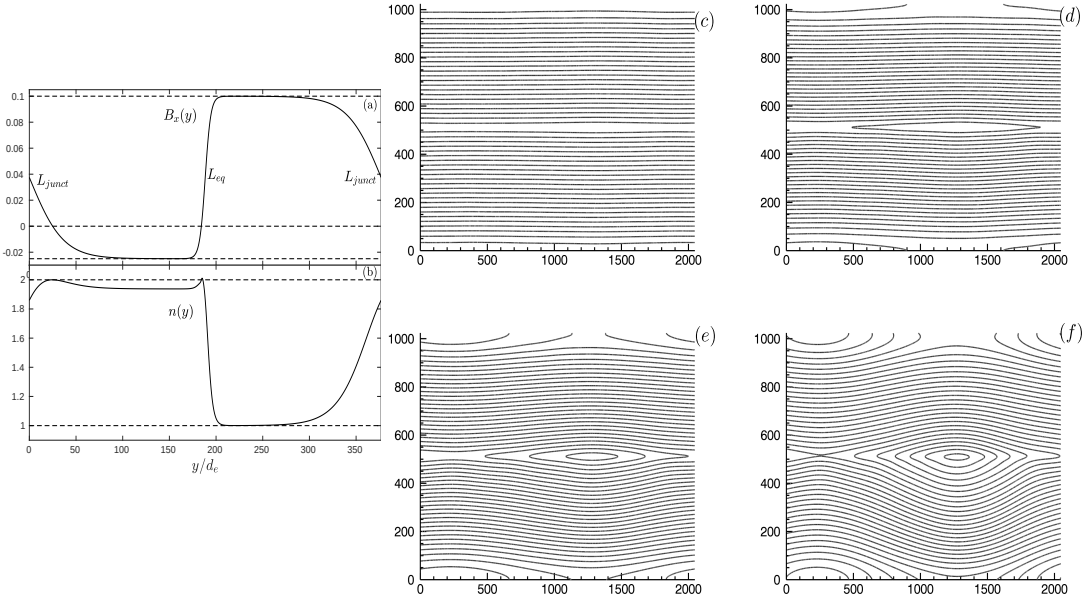

Figure 2: Left column: The magnetic and density equilibrium profile, top and bottom frames, respectively. Central and right columns: The flux function ψ in the (x, y) plane at $t = 0, 100$ and $t = 150, 200$, first and second row, respectively

crucial to be immediately in the conditions for starting the project. Thanks to this grant, we have been able to obtain intense computational resources by applying to a INAF A project and to a ISCRA B project. This initial phase of the project has been very fruitful thus giving us the possibility to start a long duration research project. It is reasonable to forecast to apply in future for a PRACE project after full optimization of the code and after having obtained results about the quality and efficiency of the numerical model in the 2D-3V limit. We are pleased to acknowledge INAF for the computational grants B that allowed us to obtain the results presented here. FC is very pleased to acknowledge Carlo Cavazzoni and Massimiliano Guarrasi (Cineca) for the support in parallelizing and optimizing the code and for technical support on Marconi KNL.

[1] A. Mangeney, F. Califano, C. Cavazzoni, and P. Travnicek, J. Comput. Phys. **179**, 495 (2002)
[2] M.R. Gibbons, D.W. Hewett, The Darwin Direct Implicit Particle-in-Cell Method for Simulation of Low Frequency Plasma Phenomena, J. Comput. Phys. **179**, 495 (2002)
[3] R. Peyret and T. D. Taylor, *Computational Methods for Fluid Flow* (Springer, New York, 1983)
[4] H. Schmitz and R. Grauer, J. Comput. Phys. **214**, 738–756 (2006)
[5] O. Pezzi et al., ..., in preparation
[6] F. Valentini, P. Travnicek, F. Califano, P. Hellinger, and A. Mangeney, J. Comput. Phys. **225**, 753 (2007)
[7] S. S. Cerri, P. Henri, F. Califano, D. Del Sarto, M. Faganello and F. Pegoraro, Physics of Plasmas, **20**, 11 (2013)